


**RESEARCH ARTICLE**

# Artificially altered gravity elicits cell homeostasis imbalance in planarian worms, and cerium oxide nanoparticles counteract this effect

Alessandra Salvetti<sup>1</sup> | Andrea Degl'Innocenti<sup>2</sup> | Gaetana Gambino<sup>1</sup> |  
 Jack J.W.A. van Loon<sup>3,4</sup> | Chiara Ippolito<sup>5</sup> | Sandra Ghelardoni<sup>6</sup> | Eric Ghigo<sup>7,8</sup> |  
 Luca Leoncino<sup>9</sup> | Mirko Prato<sup>10</sup> | Leonardo Rossi<sup>1</sup> | Gianni Ciofani<sup>2</sup> 

<sup>1</sup>Università di Pisa, Department of Clinical and Experimental Medicine, Biology and Genetics unit, Pisa, Italy

<sup>2</sup>Istituto Italiano di Tecnologia, Center for Materials Interfaces, Smart Bio-Interfaces, Pisa, Italy

<sup>3</sup>Dutch Experiment Support Center (DESC), Department of Oral and Maxillofacial Surgery/Oral Pathology, Amsterdam UMC location VU University Medical Center & Academic Centre for Dentistry Amsterdam (ACTA), Amsterdam, The Netherlands

<sup>4</sup>TEC-MMG LIS lab, European Space Agency (ESA), European Space Research and Technology Center (ESTEC), Noordwijk, The Netherlands

<sup>5</sup>Department of Clinical and Experimental Medicine, Biology and Genetics Unit, Università di Pisa, Pisa, Italy

<sup>6</sup>Department of Pathology, Biochemistry Unit, Università di Pisa, Pisa, Italy

<sup>7</sup>Institut Hospitalo-Universitaire Méditerranée Infection, Marseille, France

<sup>8</sup>Techno Jouvence, Marseille, France

<sup>9</sup>Istituto Italiano di Tecnologia, Electron Microscopy Facility, Genoa, Italy

<sup>10</sup>Istituto Italiano di Tecnologia, Materials Characterization Facility, Genoa, Italy

**Correspondence**

Alessandra Salvetti, Università di Pisa,  
 Department of Clinical and Experimental  
 Medicine, Biology and Genetics unit, Via  
 Alessandro Volta 4, 56126 Pisa, Italy.  
 Email: alessandra.salveti@unipi.it

Gianni Ciofani, Istituto Italiano di Tecnologia,  
 Center for Materials Interfaces, Smart Bio-  
 Interfaces, Viale Rinaldo Piaggio 34, 56025  
 Pontedera, Pisa, Italy.  
 Email: gianni.ciofani@iit.it

**Funding information**

European Space Agency, Grant/Award  
 Number: CORA-GBF-2017-001

**Abstract**

Gravity alterations elicit complex and mostly detrimental effects on biological systems. Among these, a prominent role is occupied by oxidative stress, with consequences for tissue homeostasis and development. Studies in altered gravity are relevant for both Earth and space biomedicine, but their implementation using whole organisms is often troublesome. Here we utilize planarians, simple worm model for stem cell and regeneration biology, to characterize the pathogenic mechanisms brought by artificial gravity alterations. In particular, we provide a comprehensive evaluation of molecular responses in intact and regenerating specimens, and demonstrate a protective action from the space-apt for nanotechnological antioxidant cerium oxide nanoparticles.

**KEYWORDS**

cerium oxide nanoparticles, hypergravity, microgravity, planarians, stem cells

Alessandra Salvetti and Andrea Degl'Innocenti contributed equally to this study.

Leonardo Rossi and Gianni Ciofani contributed equally to this study.

This is an open access article under the terms of the Creative Commons Attribution-NonCommercial License, which permits use, distribution and reproduction in any medium, provided the original work is properly cited and is not used for commercial purposes.

© 2021 The Authors. *Journal of Biomedical Materials Research Part A* published by Wiley Periodicals LLC.

## 1 | INTRODUCTION

Gravity is an environmental parameter that has constantly influenced the evolution of life on Earth, promoting the development of specific structures such as the skeletal, circulatory and muscle apparatuses, and affecting several biological processes including embryogenesis and organ physiology.<sup>1</sup> Although frog (*Xenopus laevis*) embryos develop properly under altered gravity,<sup>2</sup> mouse embryos do not,<sup>3</sup> and newt (*Pleurodeles walt*) embryos develop with neural tube defects,<sup>4</sup> regenerating abnormal curved tail.<sup>5</sup> Microgravity stimulates cell growth,<sup>6</sup> affects the beating frequency of cardiomyocytes,<sup>7</sup> and enhances differentiation of mesenchymal stem cells.<sup>8-10</sup> Hypergravity influences longevity in *Drosophila*,<sup>11</sup> and increases proliferation and differentiation of bone marrow stromal progenitors.<sup>12</sup> Moreover, several studies demonstrate that altered gravity affects signaling pathways<sup>13-16</sup> and modifies the transcriptional profile of factors not exclusively associated with stress response.<sup>10,17-22</sup> The understanding of the biological effects produced by altered gravity conditions is a relevant issue for spaceflight, bearing in mind that – after long-term missions – astronauts experience a number of health problems, like atrophy of muscles, bone demineralization, cardiopulmonary, ocular and vestibular complications, and modifications in the nervous system connections.<sup>23-26</sup> Special challenges are to be faced when attempting to study altered gravity on a whole organism, and therefore our knowledge about the effects of gravity perturbations in vivo is still scarce and fragmented. Using simple worms (planarians, Platyhelminthes) as a model system, we simulated altered gravity conditions by using a large diameter centrifuge (LDC) and a random positioning machine (RPM) at the European Space Research and Technology Centre of the European Space Agency (ESA-ESTEC) ground-based facilities, in Noordwijk, the Netherlands. Our aim is to gain insight about the potential effects of altered gravity on stem cell proliferation, differentiation and homing, as well as tissue and organ morphogenesis. Aspects making planarians apt for our study reside in their outstanding capacity of regeneration, a process in which planarian stem cells – the neoblasts – proliferate and accumulate beneath a wound surface producing a blastema, a region in which missing body structures are rebuilt through the activation of complex developmental processes.<sup>27,28</sup> The availability of numerous experimental techniques and cell- or tissue-specific molecular markers make planarians a sound system for in vivo studies.<sup>29-35</sup>

Recently, planarians have also been proposed as a model for space biology. A few papers report about how altered gravity influences planarian locomotion, asexual reproduction and transcriptional profile. In particular, the effects on tissue regeneration change in dependence of different experimental designs and conditions.<sup>36-38</sup> Thus, a more systematic approach and additional investigations are needed to discover the impact of gravity on de novo tissue morphogenesis. In this respect, we provide comprehensive information on the biological response to simulated hyper- and microgravity in both intact and regenerating planarians, and propose a model in which reactive oxygen species (ROS) are the underlying cause of cell homeostasis unbalance produced by altered gravity. Indeed, pre-treatment

of animals exposed to artificially altered gravity with cerium oxide nanoparticles (CONPs), biocompatible and long-lasting ROS scavengers that mimic endogenous antioxidants like catalase and superoxide dismutase,<sup>39,40</sup> counteracts such homeostasis unbalance in all tested altered gravity conditions.

## 2 | MATERIALS AND METHODS

### 2.1 | Animals

The asexual strain GI of the planarian *Dugesia japonica* (Tricladida Dugesidae)<sup>41</sup> was bred in artificial water (CaCl<sub>2</sub> 2.5 mM, NaHCO<sub>3</sub> 0.8 mM, MgSO<sub>4</sub> 0.4 mM, KCl 0.077 mM in distilled water) at 18°C.<sup>42</sup> Planarians were transferred to ESA-ESTEC, in Noordwijk (The Netherlands), in boxes filled with artificial water at the temperature of about 22°C. They were used for experiments after 24 h of acclimation and 2 weeks of fasting. Planarians are non-cephalopod invertebrates, and all animal experiments were performed in agreement with Italian and European law, as well as with guidelines and recommendations of the Federation of European Laboratory Animal Science Associations (FELASA).

### 2.2 | Nanoparticle characterization

A single source of CONPs (1406RE, Nanostructured & Amorphous Materials, Inc., Houston) was utilized throughout all experimental procedures. To characterize nanoparticle morphology, size and crystalline structure, micrographs of CONPs were taken via transmission electron microscopy (TEM), utilizing a JEM-1400Plus microscope with thermionic source (LaB<sub>6</sub>), operated at 120 kV, equipped with a Gatan CCD camera Orius 830 (2048 × 2048 active pixels). Images were collected with two different modalities, namely in bright field (BF) and in selected area aperture diameter (SAED, approximately 5.25 μm). Water suspensions of CONPs for TEM analyses were prepared as follows: CONPs were suspended in ultra-pure water, sonicated with ultrasound, loaded onto an ultrathin carbon film on Cu grid, and dried in low vacuum at room temperature.

X-ray photoelectron spectroscopy (XPS) analysis was carried out to evaluate the chemical state of the CONPs used in the experiments, with a particular focus on assessing the Ce<sup>3+</sup> and Ce<sup>4+</sup> contents. The specimen for XPS analysis was prepared by pressing a few milligrams of finely ground CeO<sub>2</sub> powder onto a high purity indium pellet (Sigma-Aldrich). Measurements were conducted on a Kratos Axis Ultra<sup>DLD</sup> spectrometer (Kratos Analytical Ltd.) using a monochromatic Al Kα source ( $h\nu = 1,486.6$  eV) operated at 20 mA and 15 kV. Wide scans were collected at pass-energy of 160 eV and energy step of 1 eV, while high-resolution spectra were collected at pass-energy of 10 eV and energy step of 0.1 eV. The Kratos charge neutralizer system was used for all the measurements. Spectra were analyzed with CasaXPS software (Casa Software, Ltd., version 2.3.22).

To determine the size distribution profile of CONPs, nanoparticles were dispersed to 1 mg/ml, together with 1 mg/ml gum Arabic (GA, G9752, Sigma-Aldrich) in planarian artificial water, and gently sonicated. We then performed dynamic light scattering (DLS) and Z-potential measurements (at 20°C), using a Zeta-sizer NanoZS 90 instrument (Malvern Instruments Ltd.). Both polydispersity index (PDI) and Z-potential were measured as average  $\pm$  standard deviation of three measurements, each consisting of 15 runs.

### 2.3 | Cerium oxide nanoparticle treatment

CONPs used in this research underwent extensive characterization in previous works, for example,<sup>39</sup> and were already used successfully in planarians without any particular adverse effects.<sup>43,44</sup> CONPs at 1 mg/ml were dispersed through a mild sonication with a probe sonicator (GM mini20 Bandelin Sonopuls, Bandelin), 5 min at 8 W, in a GA 1 mg/ml dispersion in artificial water. For controls, GA-only dispersions were prepared following the same procedures. GA is the vehicle in which CONPs are dispersed and it has no effect on planarian tissue regeneration and stem cell biology.<sup>44</sup> CONP treatment was performed following the experimental conditions described in<sup>43,44</sup> at which its internalization in the cytoplasm of planarian cells has been demonstrated. Briefly, animals were immersed for 24 h in CONP or GA-only medium and then rinsed 3 times with 50 ml of artificial water to completely wash out CONPs and GA.

### 2.4 | Simulated altered gravity experiments

The large diameter centrifuge (LDC)<sup>45</sup> (Figure 1(a)) was used at 10 g for simulated hypergravity experiments. Simulated microgravity was achieved via a random positioning machine (RPM; Dutch Space/EADS) at 30°/s (Figure 1(b)).<sup>46,47</sup> The RPM was used with a maximum random speed of 30°/s, random direction and interval. The samples were never more than 10 cm away from the center of

rotation. Both kinds of experiments were invariably carried out at 18°C. For 1 g control, animals were simply left at 18°C for the appropriate amount of time in parallel with the LCD or RPM run. Groups of 10 planarians were put in 50 ml falcon tubes, filled out completely with artificial water. Those for RPM experiments were especially inspected to make sure that no visible air bubbles formed after caps were screwed on securely. Two independent runs (run 1 and run 2) were performed for each experimental condition at a distance of 2 days (experiments of exposition to altered gravity for 6 and 24 h) or 3 days (experiments of exposition to altered gravity for 60 h) (Figure 2).

### 2.5 | Morphometric analysis of blastema size

Immediately before to enter LDC or RPM, GA-, and CONPs-treated animals were cut between auricles and pharynx, producing head (tail-regenerating), and tail (head-regenerating) fragments. Fragments were then exposed to simulated altered gravity for 6 or 60 h and fixed as previously described<sup>48</sup> at 60 h after cut, namely immediately at the end of a 60-h run or after 54 h from a 6-h run. Controls (1 g) were processed analogously. Samples were examined under a stereomicroscope (Stemi 305, Carl Zeiss Microscopy GmbH), equipped with a camera (Axiocam Erc 5 s, Carl Zeiss Microscopy GmbH). Digital images were quantified using Image J software.<sup>49</sup> For each animal, blastema and total body area were measured for at least 15 regenerating animals for each experimental group. We considered as blastema the unpigmented region below the wound epithelium; blastemal margin was manually highlighted by the operator in blind. The total body area was approximated to the area of the rectangle drawn around the body margin.

### 2.6 | Whole-mount in situ hybridization

DNA template for *NB.21.11.e*, a marker for early stem cell progeny,<sup>50</sup> was produced as previously described.<sup>51</sup> Digoxigenin (DIG)-labeled

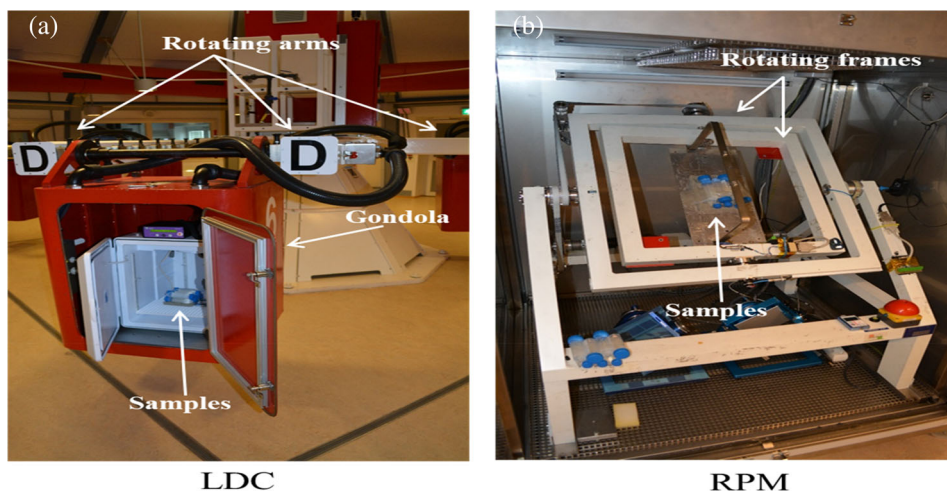


**FIGURE 1** Ground-based facilities at ESTEC. (a) LDC used at 10 g for simulated hypergravity. (b) RPM, used with a setting of maximum speed of 30°/s for simulated microgravity

RNA probe was obtained by in vitro transcription of the purified template using DIG-labelling mix (Roche Applied Science). 60 h after exposure to altered gravity, intact animals were fixed and treated for

whole-mount in situ hybridization (WISH) as previously described.<sup>52</sup> After colorimetric development, samples were dipped in 50% glycerol/10% methanol, and analyzed under the stereomicroscope.

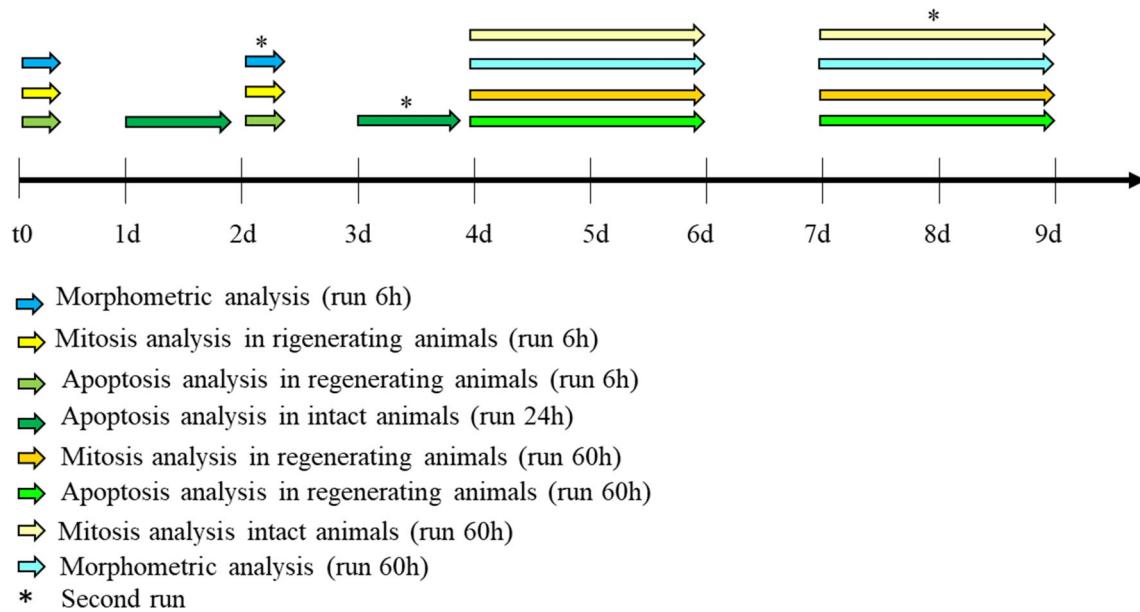


**FIGURE 2** Overall study overview. Schematic representation including all experimental groups and times of run 1 and run 2

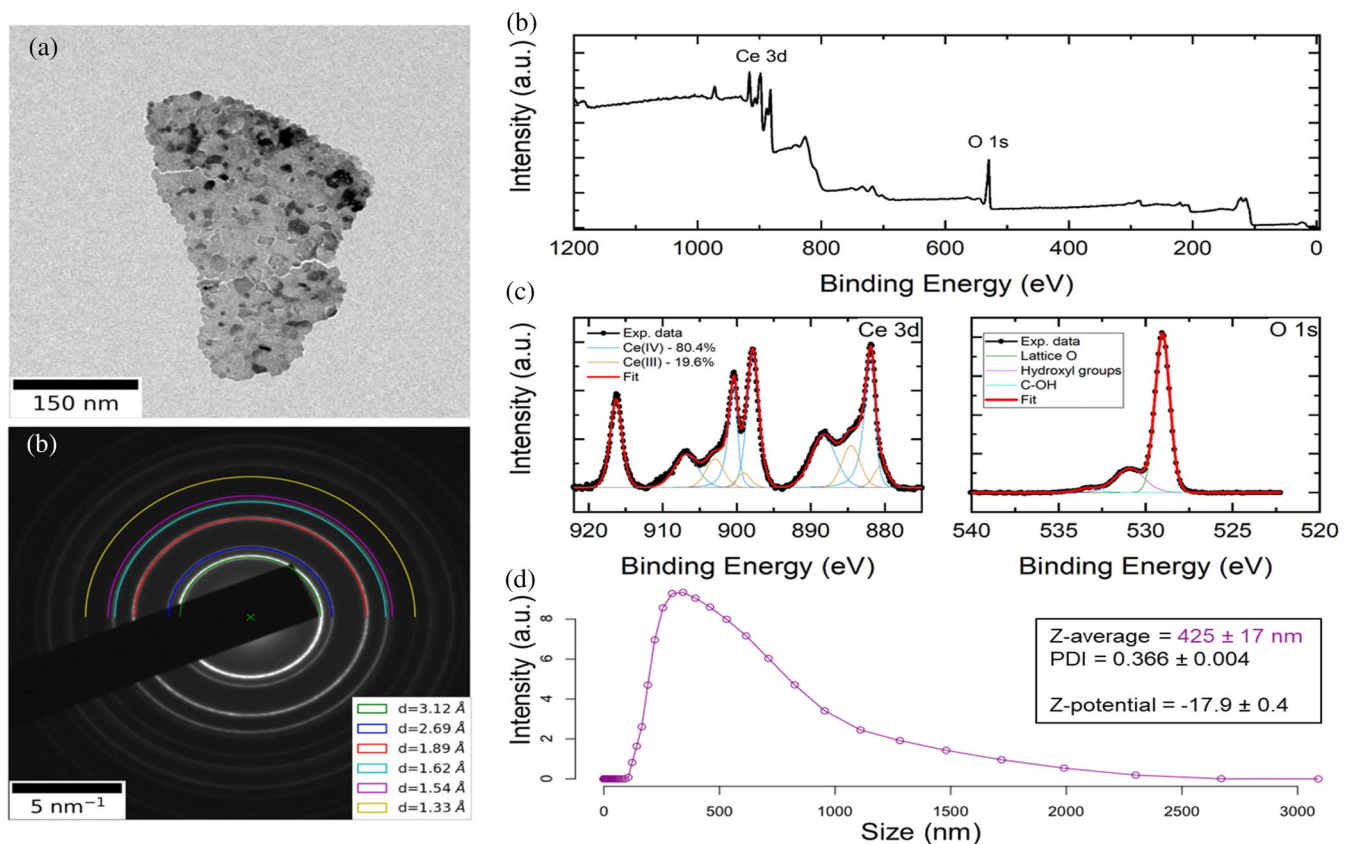


**FIGURE 3** Cerium oxide nanoparticle characterization. (a) Representative TEM image. (b) Diffraction pattern, showing crystalline structure. (c) XPS wide scan. (d) High-resolution spectra collected on the Ce 3d and O 1s energy regions. High resolution data are shown together with the results of the best fit procedure. (e) DLS measurements, with size distribution; PDI, Z-average and Z-potential indicated in the box as mean values ± standard deviation



NB.21.11.e signal was quantified as already described.<sup>53</sup> Briefly, each animal was photographed at the same magnification and exposition; pictures were then converted into grayscale mode and inverted. The mean gray value (raw intensity/animal area) was recorded by the ImageJ software. Mean gray recorded from animals ( $n = 10$ ) belonging to the same experimental class was utilized to obtain the mean gray value of the group.

## 2.7 | Terminal deoxynucleotidyl transferase dUTP nick end labeling

Terminal deoxynucleotidyl transferase dUTP nick end labeling (TUNEL) assay was performed by using ApopTag Red in situ apoptosis detection kit (EMD Millipore Corporation) as previously described.<sup>48</sup> Stained animals were mounted in 80% glycerol, and analyzed using a confocal microscope (TCS SP8, Leica Microsystems CMS) by tile scan

function and zeta-stack optical sectioning every 2  $\mu\text{m}$ , respectively. Five planarians were analyzed for each experimental condition. A single composite image was taken for each specimen. The number of apoptotic cells in intact and regenerating (60 h of simulated altered gravity regime) animals was evaluated using the "find maxima" option of the Image J software and normalized versus the animal body area. In the case of regenerating animals exposed to artificially altered gravity for 6 h, the number of apoptotic cells was exclusively counted in 100  $\mu\text{m}$  tissue strip from the amputation site.

## 2.8 | Western blotting

Mitotic cells were quantified using the mitotic marker phosphohistone H3 antibody (H3P Ab, O6-570, Sigma-Aldrich) by Western blotting. Nine animals for each experimental class were amputated and immediately exposed to artificially altered gravity for 6 or 60 h.

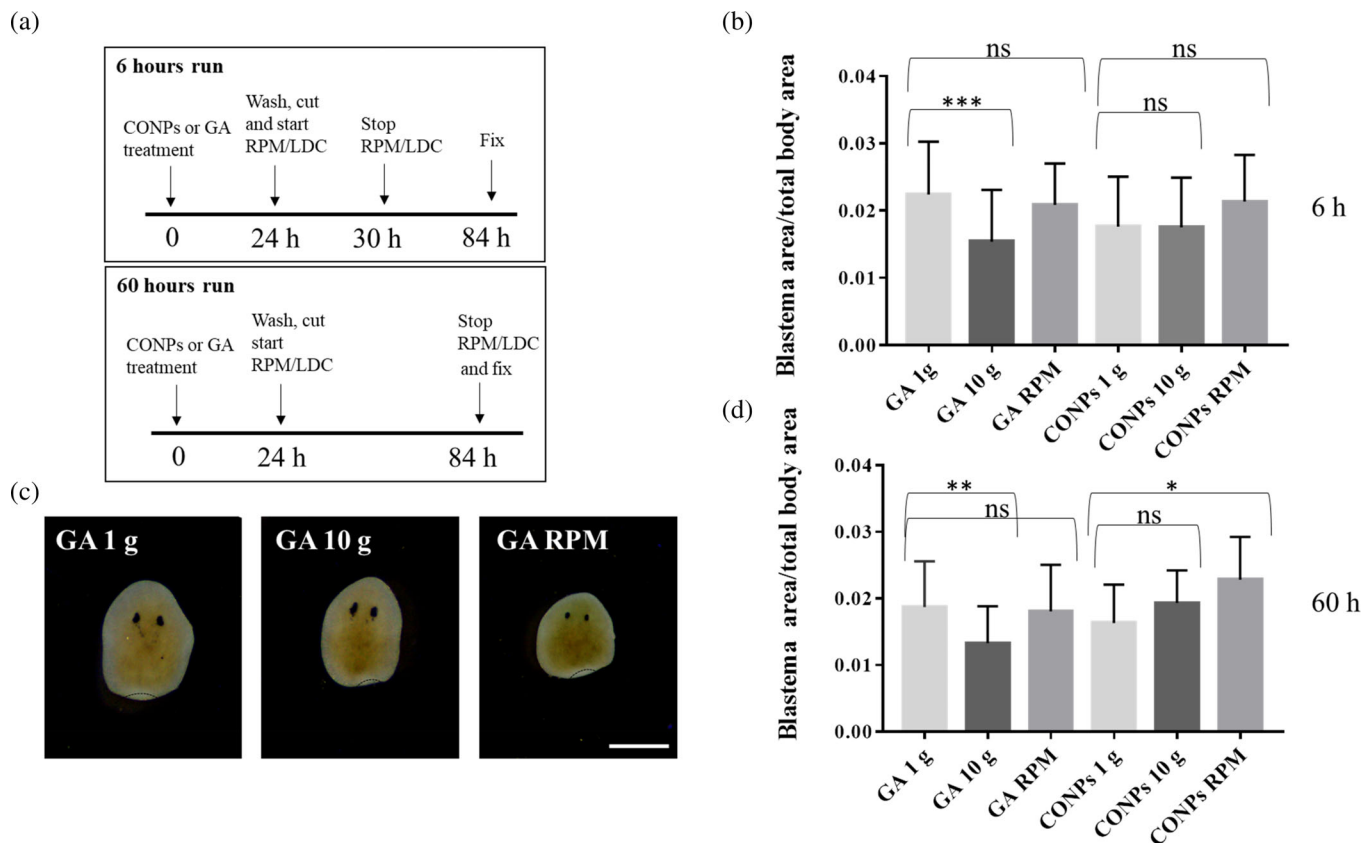


**FIGURE 4** Morphometric analysis of head blastema in animals pre-treated with cerium oxide nanoparticles (CONPs) or gum Arabic (GA) and exposed to different gravity regimes. (a) Schematic representation of the experimental set-up. (b) Representative head fragments regenerating a tail exposed to 1 g (GA 1 g), hypergravity (GA 10 g), or artificial microgravity (GA RPM). The blastema is marked by black dots. Scale bar is 500  $\mu\text{m}$ . (c) Morphometric analysis of blastemal area after 6 h of exposure to different gravity regimes, in GA-treated animals exposed to 1 g (GA 1 g), hypergravity (GA 10 g), simulated microgravity (GA RPM) and in CONPs-treated animals exposed to 1 g (CONPs 1 g), hypergravity (CONPs 10 g), or simulated microgravity (CONPs RPM). Each bar is the mean  $\pm$  standard deviation of 15 independent samples of run 1. Comparable results were obtained with samples of run 2. Significant differences were evaluated by unpaired Student's *t*-test analysis (\*\* $p < 0.001$ ; \* $p < 0.01$ ; ns: not significant) and two-way ANOVA. (d) Morphometric analysis of blastemal area after 60 h of exposure to different gravity regimes. Each bar is the mean  $\pm$  standard deviation of 15 independent samples of run 1. Comparable results were obtained with samples of run 2. Significant differences were evaluated by unpaired Student's *t* test analysis (\*\* $p < 0.01$ ; \* $p < 0.05$ ; ns: not significant) and two-way ANOVA

Nine intact animals were exposed to simulated altered gravity for 24 h. After exposition, three independent groups (each composed by three animals) were immediately frozen, and proteins were extracted by adding 1X Laemmli buffer (0.1% 2-mercaptoethanol, 0.0005% bromophenol blue, 10% glycerol, 2% SDS electrophoresis-grade, 63 mM Tris-HCl pH 6.8). Proteins were transferred onto nitrocellulose membrane using Mini Trans-blot electrophoretic transfer cell apparatus (Bio-Rad Laboratories Inc.) following the manufacturer's instruction. After blocking with 5% nonfat dry milk (Bio-Rad Laboratories Inc.) in PBST (0.05% Tween 20, Sigma, in PBS 1×), membranes were incubated with 1:500 of H3P antibody in 1% non-fat dry milk in PBST for 2 h. Anti- $\alpha$ -tubulin antibody, mouse monoclonal (T6199, Sigma-Aldrich) was used as loading control at 1:20000 dilution. Membranes were then washed in PBST and incubated with anti-mouse IgG horseradish peroxidase (HRP; 6,402-05, Biovision) or anti-rabbit IgG HRP (6401-05, Biovision) diluted 1:50000 in 1% nonfat dry milk in PBST for 1 h. The chemiluminescence detection was performed using the Immobilon Western chemiluminescent HRP substrate kit (Millipore Corp.) following the manufacturer's instruction. To visualize immunoblots, we used a luminescent image analyzer (Chemidoc XSR + System Bio-Rad) and the Image LabTM Software (Bio-Rad Laboratories). Only bands below the saturation limit were analyzed. The

chemiluminescence was expressed in terms of volume of specific immunoreactive bands and, in each lane, the protein level was normalized to the  $\alpha$ -tubulin level. Three technical replicates were performed for each Western blot.

## 2.9 | Statistical analysis

Unpaired Student's *t* tests ( $\alpha = 0.05$ ) and two-way ANOVA ( $\alpha = 0.05$ ) were applied to evaluate statistical significance, respectively using the software GraphPad Prism 7.00 and Free Statistics Software v1.2.1 ([https://www.wessa.net/rwasp\\_Two%20Factor%20ANOVA.wasp/](https://www.wessa.net/rwasp_Two%20Factor%20ANOVA.wasp/)).

## 3 | RESULTS

### 3.1 | Cerium oxide nanoparticle characterization

Figure 3 shows a representative TEM image of CONPs (a), the diffraction pattern of the powder (b), as well as the XPS wide scan (c), with high-resolution spectra collected on the binding energy regions typical for Ce 3d and O 1 s peaks (d).

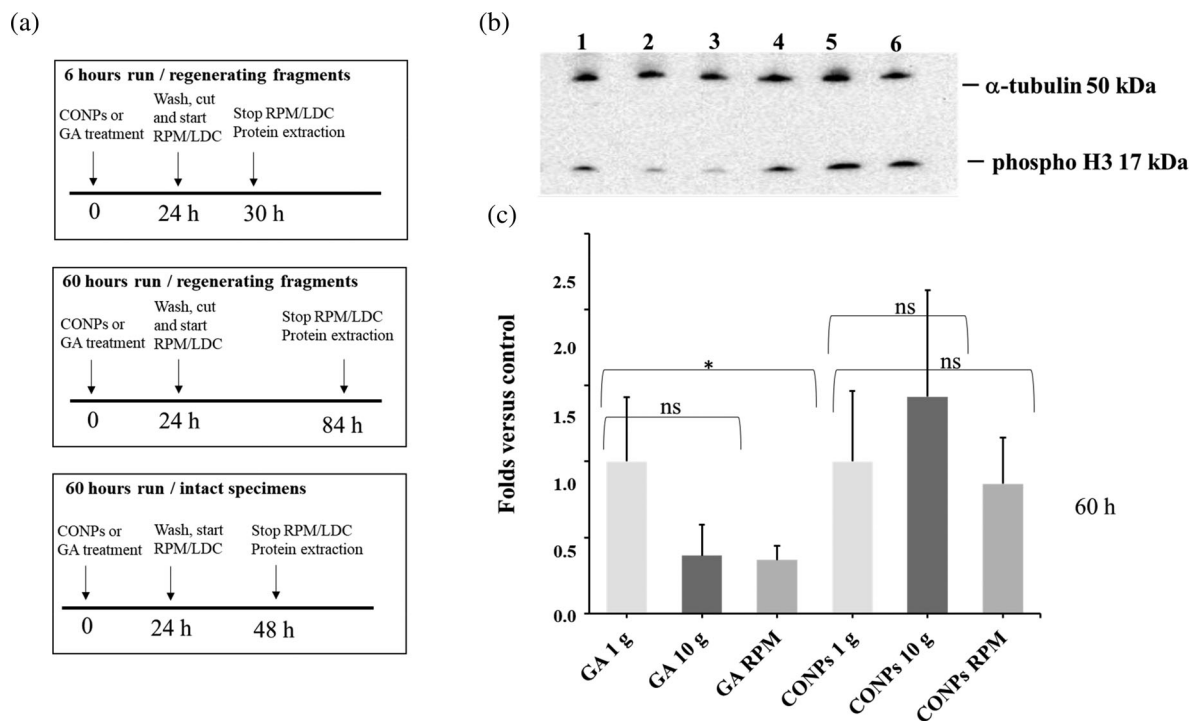


**FIGURE 5** Quantification of the mitotic marker phospho-histone H3 in animals pre-treated with cerium oxide nanoparticles (CONPs) or only gum Arabic (GA) and exposed to different gravity regimes. (a) Schematic representation of the experimental set-up. Numbers indicate hours (h). (b) Representative Western blotting. Lane 1: GA-treated animals at 1 g; lane 2: GA-treated animals at 10 g; lane 3: GA-treated animals exposed to artificial microgravity; lane 4: CONPs-treated animals at 1 g; lane 5: CONPs-treated animals at 10 g; lane 6: CONPs-treated animals exposed to simulated microgravity. (c) Quantification of mitotic cells. GA-treated animals exposed to 1 g (GA 1 g), 10 g (GA 10 g), or simulated microgravity (GA RPM); CONPs-treated animals exposed to 1 g (CONPs 1 g), 10 g (CONPs 10 g), or simulated microgravity (CONPs RPM). Each bar is the mean  $\pm$  standard deviation of three independent samples, for each experimental group, of run 1, normalized versus the corresponding GA control, to which an arbitrary value of 1 was attributed. Comparable results were obtained with samples of run 2. Significant differences were evaluated by unpaired Student's *t* test analysis (\* $p < 0.05$ ; ns: not significant) and two-way ANOVA. Each Western blotting has been performed in triplicate

Powder electron diffraction pattern show sharp diffraction rings indicating that the nanoparticles have a crystalline nature compatible with that one of cubic ceria.<sup>54</sup>

Concerning XPS, From the wide scan we could confirm the high purity of the nanomaterial, as the observed peaks could all be assigned to either cerium or oxygen, a part from a low intensity carbon peak at  $\sim 285$  eV, partially overlapping with Ce 4 s ones. The high-resolution spectra are shown after background subtraction, together with the outcome of the fitting procedure. The best fit on the Ce 3d spectrum was obtained with five sets of spin-orbit split doublets, three of which representative of Ce(IV) (light blue profiles in the figure) and two of Ce(III) (orange profiles) oxides, as described in.<sup>55</sup> The splitting between the two components of each doublet has been set to 18.6 eV, as reported in,<sup>56</sup> while the intensity ratio between the two components is set to 3:2, due to spin-orbit coupling. The relative content of Ce<sup>3+</sup> and Ce<sup>4+</sup> species in the sample was calculated from the ratio of the sum of the integrated areas of the XPS 3d peaks related to the two oxidation states to the total integral area for the whole Ce 3d region. The acquired XPS spectrum is consistent with a Ce<sup>3+</sup> percent concentration of  $19.6 \pm 2.0\%$  (Ce<sup>4+</sup>  $80.4 \pm 2.0\%$ ), corresponding to a Ce<sup>3+</sup>/Ce<sup>4+</sup> ratio of about 0.24. The O 1 s spectrum was fitted with three peaks. The main one, centered at  $529.0 \pm 0.2$  eV, corresponds to lattice oxygen in CeO<sub>2</sub>, in agreement with the literature.<sup>57</sup> To obtain the best fit, two low intensity peaks were centered at  $530.9 \pm 0.2$  eV and  $533.3 \pm 0.2$  eV, and are assigned to hydroxides and C—OH groups at the surface of the CONPs.<sup>57</sup> DLS measurements (Figure 3(e)) are in line with our previous reports,<sup>43</sup> namely an hydrodynamic size of  $425 \pm 17$  nm, a PDI of  $0.366 \pm 0.004$ , and a Z-potential of  $-17.9 \pm 0.4$  mV.

### 3.2 | Altered gravity and tissue regeneration

With the aim to understand the effect of gravity on tissue regeneration, we performed a morphometric analysis of 3-day-old blastema area of planarians exposed to simulated altered gravity, with or without previous treatment with CONPs and according to the experimental design depicted in Figure 4(a). In order to normalize differences in blastema area that might depend on the use of animals of different sizes, we initially investigated the dependence of these two variables. Regression analysis of blastema area with respect to body area, performed throughout the dataset, shows a linear correlation ( $R = 0.7$ , significance F close to 0). For this reason, we chose the ratio between blastema area and total body area as the most appropriate parameter to evaluate effects on tissue regeneration. Our data indicate that 6 or 60 h exposition to simulated hypergravity produced a significant reduction in the head fragment regeneration, and this reduction was rescued by CONP treatment (Figure 4(b)-(d) and Figure S1). RPM did not affect tissue regeneration at both 6 and 60 h, and CONP supplementation slightly increases the process at 60 h (Figure 4(c)-(d), and Figure S1). No statistically significant differences were detected between groups for tail fragments (Figure S2a-b).

### 3.3 | Altered gravity and cell proliferation rate

To assess the effect of altered gravity on cell proliferation, we analyzed the expression of phospho-histone H3, a marker of mitosis, in regenerating and intact animals treated with CONPs or GA according

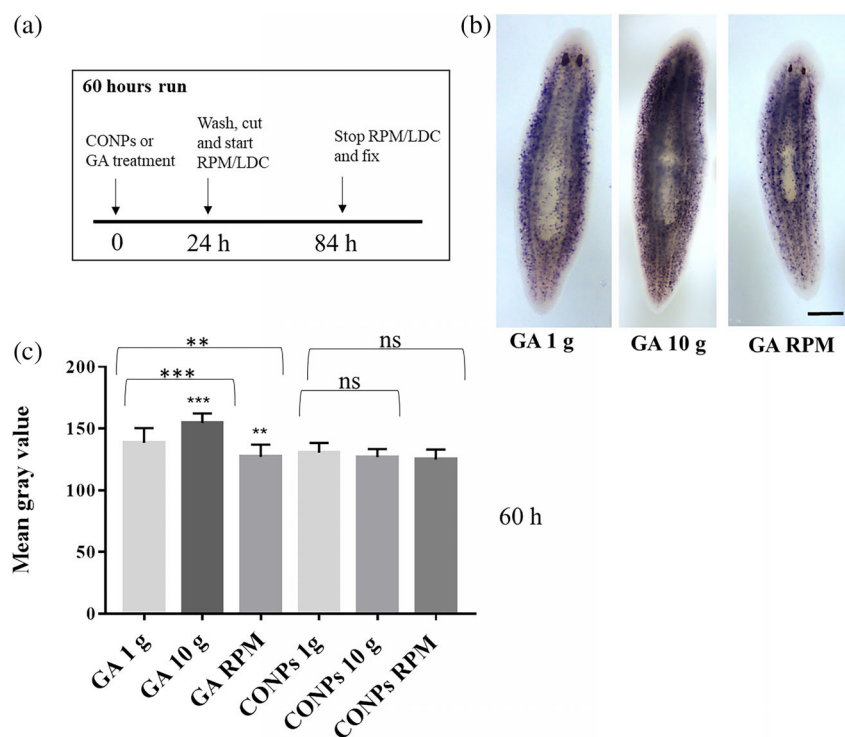


**FIGURE 6** Analysis of the expression of NB-21.11.e, a marker of early progeny, in animals pretreated with gum Arabic (GA) or cerium oxide nanoparticles (CONPs) and exposed for 60 h at different gravity regimes. (a) Schematic representation of the experimental set-up. Numbers indicate hours (h). (b) Representative images of NB-21.11.e expression by whole-mount in situ hybridization (WISH) in a GA-treated animal exposed to 1 g (GA 1 g), 10 g (GA 10 g) or simulated microgravity (GA RPM). Scale bar is 500  $\mu$ m. (c) Quantification of signal intensity detected by WISH. Each bar is the mean value  $\pm$  standard deviation of the mean gray values measured in ten independent samples, for each experimental group, of run 1. Comparable results were obtained with samples of run 2. Significant differences were evaluated by unpaired Student's t test analysis (\*\* $p < 0.01$ ; \*\*\* $p < 0.001$ ; ns: not significant) and two-way ANOVA

to the experimental design indicated in Figure 5(a). We did not detect significant changes in the expression of the mitotic marker in both intact animals (exposed to simulated altered gravity for 60 h; Figure S2c) and in regenerating fragments exposed to artificially altered gravity for only 6 h (Figure S2d). On the contrary, a significant reduction in the number of mitotic cells in regenerating fragments exposed to RPM for 60 h was detectable. A similar trend, although not statistically significant, was also detectable in regenerating fragments exposed for 60 h to artificial hypergravity ( $p$  value from 0.05 to 0.1 for the different technical replicates; Figure 5(b)-(c) and Figure S1). Pre-treatment of animals with CONPs induced a rescue in animals exposed to simulated altered gravity with respect to the control (Figure 5(b)-(c) and Figure S1).

### 3.4 | Altered gravity and cell differentiation

To understand the effect of simulated altered gravity on cell commitment, we analyzed the expression of *NB.21.11.e*, a marker of early neoblast progeny towards epidermal cell lineage, by WISH experiments performed on intact planarians exposed to artificially altered gravity for 60 h with or without previous treatment with CONPs

(Figure 6(a) and Figure S1). In particular, we exposed animals to altered gravity for 60 h and sacrificed them, a time point at which the effect can be evaluated on early epidermal progeny.<sup>50</sup> We found that *NB.21.11.e* expression is increased upon simulated hypergravity and reduced upon simulated microgravity (Figure 6(b)-(c) and Figure S1). These differences were not detectable in animals treated with CONPs (Figure 6(b)-(c) and Figure S1).

### 3.5 | Altered gravity and cell death

The effect of altered gravity on cell death was analyzed by whole-mount TUNEL assay in intact planarians and regenerating fragments at 6 and 60 h after amputation. We detected a significant increase in the number of apoptotic cells in intact animal treated with GA and exposed to simulated altered gravity for 24 h (Figure 7 and Figure S1). The number of apoptotic cells clearly increased 6 h after amputation in animals exposed to artificial hypergravity with respect to controls, while it also resulted in a significant reduction in animals in the RPM (Figure 8 and Figure S1). No difference was observed in animals exposed to altered gravity after 60 h of regeneration (Figure S2e). The treatment of both intact and regenerating animals with CONPs

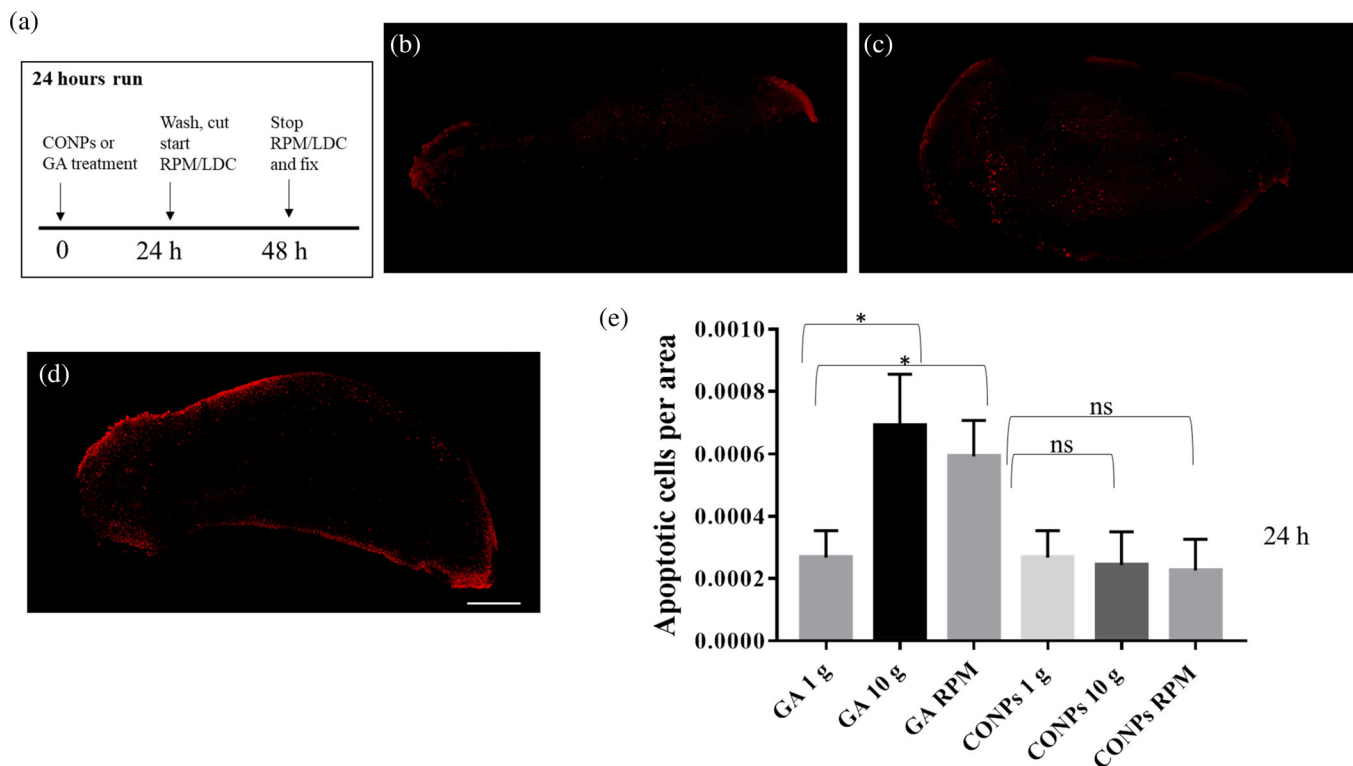


**FIGURE 7** Analysis of apoptotic cells by TUNEL assay in intact animals after 24 h of altered gravity. (a) Representation of the experimental set-up. Numbers indicate hours (h). (b-d) Confocal representative images of apoptotic cells (red dots) in animals treated with Gum Arabic (GA) and exposed to (b) 1 g (GA 1 g), (c) hypergravity (GA 10 g) or (d) simulated microgravity (GA RPM). Scale bar is 100  $\mu$ m. (e) Quantification of apoptotic cells in animals exposed to altered gravity in presence of GA or cerium oxide nanoparticles (CONPs). CONPs-treated animals exposed to 1 g (CONPs 1 g), hypergravity (CONPs 10 g) or simulated microgravity (CONPs RPM). Each bar is the mean  $\pm$  standard deviation of three independent samples of run 1. Comparable results were obtained with samples of run 2. Significant differences were evaluated by unpaired Student's  $t$  test analysis ( $*p < 0.05$ ; ns: not significant) and two-way ANOVA



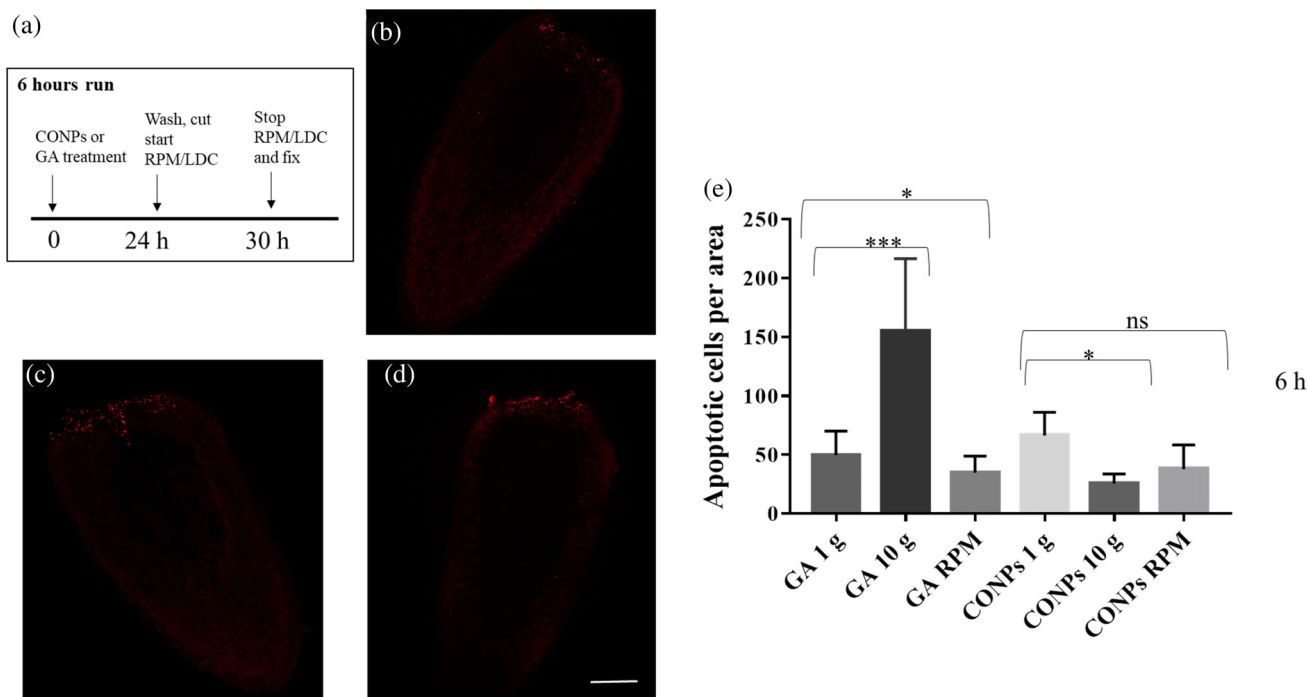


**FIGURE 8** Analysis of apoptotic cells by TUNEL assay in regenerating planarians 6 h after amputation. (a) Representation of the experimental set-up. Numbers indicate hours (h). (b–d) Confocal representative images of TUNEL positive-cells (red dots) in animals treated with Gum Arabic (GA) exposed to (b) 1 g (GA 1 g), (c) hypergravity (GA 10 g), (d) simulated microgravity (GA RPM). Scale bar is 100  $\mu$ m. (e) Quantification of apoptotic cells in animals exposed to 6 h altered gravity in presence of GA or cerium oxide nanoparticles (CONPs). CONPs-treated animals exposed to 1 g (CONPs 1 g), 10 g (CONPs 10 g) or simulated microgravity (CONPs RPM). Each bar is the mean  $\pm$  standard deviation of five independent samples of run 1. Comparable results were obtained with samples of run 2. Significant differences were evaluated by unpaired Student's *t* test analysis (\*\**p* < 0.001; \**p* < 0.05; ns: not significant) and two-way ANOVA

counteracted the alteration in the number of apoptotic cells (Figure 7-8 and Figure S1).

## 4 | DISCUSSION

Planarians are extremely resilient to the perturbation of cell homeostasis processes, including traumatic events such as extensive tissue damage. Their sturdiness resides in the adaptive response of a plastic body where homeostatic processes are continuously adjusted by cross-talk between stem cells and differentiated body parts, which have been suggested to represent a global stem cell niche.<sup>31</sup> For these reasons, unbalancing regenerative and homeostatic performances of planarians is challenging. Accordingly, artificially altered gravity did not permanently perturb planarian regeneration even in extreme conditions. Indeed, animals were able to complete a functional regeneration, although we observed a reduced regenerative capability in head fragments following exposure to simulated hypergravity. Higher susceptibility of head fragments – with respect to tail fragments – to factors perturbing stem cell activity has been commonly demonstrated for these organisms.<sup>58</sup> This phenomenon is probably due to the lower number of stem cells spread in this part of the body, so that minimal variations in the number of neoblasts induce a more readily observable phenotype. In general terms, a reduction in the regeneration

ability might owe to reduced cell proliferation and/or an increased cell death. These two biological phenomena are indeed finely regulated during planarian regeneration, both showing two waves of activity, that is, one early after cut and the other later. While apoptosis and proliferation share this biphasic pattern, their distribution in the body is opposite. For apoptosis, the early peak occurs near the wound surface, and the second one is dispersed throughout the body<sup>59</sup>; the exact contrary occurs for proliferation, being mitotic cells accumulated under the growing blastema only in the second proliferation burst.<sup>60</sup> A maximal impact upon blastema growth is therefore expected in case of an increase in the first peak of apoptosis and of a decrease in the second peak of proliferation. Slight changes in the number of apoptotic or mitotic cells spread far from the regeneration site are unlikely to directly perturb blastema growth.

In all altered gravity conditions tested in this study, we monitored a reduction of the proliferative activity in the second peak, which is consistent with a reduced blastema growth. On the contrary, we monitored an increase in apoptotic cells under the wound surface in early regeneration only in artificial hypergravity conditions. In the RPM, the number of apoptotic cells localized below the wound is slightly reduced. This difference might be at the basis for the different effect upon blastema growth observed in microgravity versus hypergravity simulations. Indeed, in this latter case the combination of two adverse effects, that is a reduced proliferation at the blastema site and an increased apoptosis under the

wound surface, might concur to the slight reduction of the blastema growth rate. We currently do not know which cells underwent apoptosis, but, as at the same time (6 h) at which we observed an increase in apoptosis, we also monitored a number of mitosis comparable to controls; so, it is possible to hypothesize that this process preferentially affects post-mitotic cells. Accordingly, it has been demonstrated that the two regenerative apoptotic waves predominantly, if not exclusively, occurred in differentiated cells.<sup>59</sup> We can thus imagine that a first early consequence of hypergravity is the induction of cell-death processes: this is also in line with what we observed in intact animals, where an increment in TUNEL-positive cells was monitored after 24 h of 10 g exposure. Altered gravity is also known to influence cell determination and differentiation in different types of cells<sup>(22,61,62,63,64)</sup>, and it also has an effect on cell differentiation in planarians, a process that can be easily followed by studying differentiation towards the epidermal lineage, for which early and late molecular markers are available.<sup>50</sup> Obtained data show again an opposite effect of hypergravity and microgravity experiments. Indeed, a significant increase of NB-21.11.e-positive cells (marker for enhanced differentiation) was detectable after simulated hypergravity exposure, while its significant reduction was produced by artificial microgravity exposure indicating a possible demonstration of the gravity continuum paradigm.<sup>65</sup>

Pre-treatment with CONPs rescued the negative impact of simulated altered gravity on the blastema growth, cell proliferation, apoptosis, and cell differentiation. We can assume that protective effect is due to internalized nanoparticles, as we extensively washed planarian before exposition to altered gravity conditions. Owing to concomitance on CONP crystalline surface of both Ce<sup>4+</sup> and Ce<sup>3+</sup> states,<sup>40</sup> CONPs show self-regenerating antioxidant properties and ROS-scavenger functions, resulting into anti-inflammatory activity.<sup>66</sup> Hence, CONPs have had several biomedical applications, and showed a protective role in disorders characterized by ROS overproduction.<sup>67-69</sup> Since several literature sources report on overproduction of ROS induced by altered gravity,<sup>70-73</sup> we hypothesize that oxidative unbalance might be the principal cellular stress at which planarian cells are exposed following altered gravity, despite additional concurrent causes cannot be ruled out. Thus, we speculate that upon hypergravity exposure cells experience an increase in ROS production, to which some respond activating a cell-death program. In turn, increases in cell death may influence the cellular homeostasis of the animal, inducing premature cell differentiation and perturbing activation of neoblasts and their subsequent accumulation to form a blastema. Further experiments will be necessary to validate our hypothesis.

## 5 | CONCLUSION

Altered gravity represents one of the main challenges for space exploration. Understanding the molecular bases of the noxious effects of hyper- and microgravity is, therefore, vital. However, it is hard to perform altered-gravity research on whole organisms, and this becomes especially true for space experimental campaigns. Simpler biological models are needed.

We utilized planarians as a straightforward platform for artificially altered gravity experiments, characterizing their molecular responses to different gravity regimens. Planarians are evolutionary distant from humans, but molecular mechanisms and fundamental signaling pathways are well conserved between the two *taxa*, so that our data can be useful for translational research.

Upon exposure to altered gravity, regenerating planarians experience transient growth delays, likely due to aberrations in tissue turnover dynamics; these, in turn, depend on a combination of increased cell death and an overall reduced proliferation capacity. When CONPs are administered, such adverse phenomena become largely unapparent; given the strongly supported involvement of oxidative stress in mediating the damages of altered gravity, and considering the recognized role of CONPs as an antioxidant, we hypothesize that such rescue effects are mostly due to CONP protecting planarians from the ROS imbalance caused by the gravitational insult.

Our findings strengthen the validity of planarian worms as a suitable model for space biology, and contribute to the understanding of the effects produced by altered gravity, as well as to the future application of emerging nanomaterials in biomedicine.

## ACKNOWLEDGMENTS

We thank Dr. Maria Grazia D'Elia for assistance on Western blotting and TUNEL assay experiments. We would also like to thank the ESA-ESTEC TEC-MMG LIS Lab, especially Mr. Alan Dowson for his support in preparation and during this study.

This work has received funding from the European Space Agency (ESA) through the grant number CORA-GBF-2017-001.

## CONFLICT OF INTEREST

The authors declare no potential conflict of interest.

## DATA AVAILABILITY STATEMENT

The data that support the findings of this study are available from the corresponding author upon reasonable request.

## ORCID

Gianni Ciofani  <https://orcid.org/0000-0003-1192-3647>

## REFERENCES

1. Brown AH. The influence of gravity on the structure and functions of plant material. *Adv Space Res.* 1984;4(12):299-303.
2. Souza KA, Black SD, Wassersug RJ. Amphibian development in the virtual absence of gravity. *Proc Natl Acad Sci.* 1995;92(6):1975-1978.
3. Ruden DM, Bolnick A, Awonuga A, et al. Effects of gravity, microgravity or microgravity simulation on early mammalian development. *Stem Cells Dev.* 2018;27(18):1230-1236.
4. Gualandris-Parisot L, Husson D, Foulquier F, et al. *Pleurodeles waltl*, amphibian, Urodele, is a suitable biological model for embryological and physiological space experiments on a vertebrate. *Adv Space Res.* 2001;28(4):569-578.
5. Grigoryan EN, Dvorochkin N, Poplinskaya VA, Yousuf R, Radugina EA, Almeida EA. The effect of hypergravity on the lens, cornea and tail regeneration in Urodela. *Acta Astronaut.* 2017;138:423-433.

6. Grimm D, Bauer J, Kossmehl P, et al. Simulated microgravity alters differentiation and increases apoptosis in human follicular thyroid carcinoma cells. *FASEB J*. 2002;16(6):604-606.
7. Acharya A, Brungs S, Lichterfeld Y, et al. Parabolic, flight-induced, acute hypergravity and microgravity effects on the beating rate of human cardiomyocytes. *Cell*. 2019;8(4):352.
8. Unsworth BR, Lelkes PI. Growing tissues in microgravity. *Nat Med*. 1998;4(8):901-907.
9. Wu X, Li SH, Lou LM, Chen ZR. The effect of the microgravity rotating culture system on the chondrogenic differentiation of bone marrow mesenchymal stem cells. *Mol Biotechnol*. 2013;54(2):331-336.
10. Zarrinpour V, Hajebrahimi Z, Jafarina M. Expression pattern of neurotrophins and their receptors during neuronal differentiation of adipose-derived stem cells in simulated microgravity condition. *Iran J Basic Med Sci*. 2017;20(2):178-186.
11. Le Bourg É, Minois N, Bullens P, Bearet P. A mild stress due to hypergravity exposure at young age increases longevity in *Drosophila melanogaster* males. *Biogerontology*. 2000;1(2):145-155.
12. Markina EA, Andrianova IV, Shtemberg AS, Buravkova LB. Effect of 30-day hindlimb unloading and hypergravity on bone marrow stromal progenitors in C57Bl/6N mice. *Bull Exp Biol Med*. 2018;166(1):130-134.
13. De Groot RP, Rijken PJ, Den Hertog J, et al. Microgravity decreases c-fos induction and serum response element activity. *J Cell Sci*. 1990;97(1):33-38.
14. Kim J, Montagne K, Nemoto H, Ushida T, Furukawa KS. Hypergravity down-regulates c-fos gene expression via ROCK/rho-GTP and the PI3K signaling pathway in murine ATDC5 chondroprogenitor cells. *PLoS One*. 2017;12(9):e0185394.
15. Tan X, Xu A, Zhao T, et al. Simulated microgravity inhibits cell focal adhesions leading to reduced melanoma cell proliferation and metastasis via FAK/RhoA-regulated mTORC1 and AMPK pathways. *Sci Rep*. 2018;8(1):1-12.
16. Ivanova K, Hemmersbach R. Guanylyl cyclase-cGMP signaling pathway in melanocytes: differential effects of altered gravity in non-metastatic and metastatic cells. *Int J Mol Sci*. 2020;21(3):1139.
17. Claassen DE, Spooner BS. Impact of altered gravity on aspects of cell biology. *Int Rev Cytol*. 1994;156:301-373.
18. Hammond TG, Lewis FC, Goodwin TJ, et al. Gene expression in space. *Nat Med*. 1999;5(4):359-359.
19. Herranz R, Larkin OJ, Hill RJ, Lopez-Vidriero I, van Loon JJ, Medina FJ. Suboptimal evolutionary novel environments promote singular altered gravity responses of transcriptome during *Drosophila* metamorphosis. *BMC Evol Biol*. 2013;13(1):133.
20. Ebnerasuly F, Hajebrahimi Z, Tabaie SM, Darbouy M. Simulated microgravity condition alters the gene expression of some ECM and adhesion molecules in adipose derived stem cells. *Int J Mol Cell Med*. 2018;7(3):146-157.
21. Yatagai F, Honma M, Dohmae N, Ishioka N. Biological effects of space environmental factors: a possible interaction between space radiation and microgravity. *Life Sci Space Res*. 2019;20:113-123.
22. Acharya A, Brungs S, Henry M, et al. Modulation of differentiation processes in murine embryonic stem cells exposed to parabolic flight-induced acute Hypergravity and microgravity. *Stem Cells Dev*. 2018;27(12):838-847.
23. Clément G, Wood SJ. Motion perception during tilt and translation after space flight. *Acta Astronaut*. 2013;92(1):48-52.
24. Gunga HC, von Ahlefeld VW, Coriolano HJA, Werner A, Hoffmann U. *Cardiovascular system, red blood cells, and oxygen transport in microgravity*. Cham: Springer; 2016.
25. Diaz Artilés A, Navarro Tichell P, Perez F. Cardiopulmonary responses to sub-maximal ergometer exercise in a hypo-gravity analog using head-down tilt & head-up tilt. *Front Physiol*. 2019;10:720.
26. Pechenkova EV, Nosikova IN, Rumshiskaya AD, et al. Alterations of functional brain connectivity after long-duration spaceflight as revealed by fMRI. *Front Physiol*. 2019;10:761.
27. Rossi L, Salvetti A, Batistoni R, Deri P, Gremigni V. Planarians, a tale of stem cells. *Cell Mol Life Sci*. 2008;65(1):16-23.
28. Alessandra S, Rossi L. Planarian stem cell heterogeneity. *Stem Cells Heterogeneity-Novel Concepts*. Cham: Springer; 2019:39-54.
29. Cebrià F, Adell T, Saló E. Rebuilding a planarian: from early signaling to final shape. *Int J Dev Biol*. 2018;62:537-550.
30. Reddien PW. The cellular and molecular basis for planarian regeneration. *Cell*. 2018;175(2):327-345.
31. Rossi L, Salvetti A. Planarian stem cell niche, the challenge for understanding tissue regeneration. *Sem Cell Dev Biol*. 2019;87:30-36.
32. Barghouth PG, Thiruvalluvan M, LeGro M, Oviedo NJ. DNA damage and tissue repair: What we can learn from planaria. *Sem Cell Dev Biol*. 2019;87:145-159.
33. Dattani A, Sridhar D, Aboobaker AA. Planarian flatworms as a new model system for understanding the epigenetic regulation of stem cell pluripotency and differentiation. *Sem Cell Dev Biol*. 2019;87:79-94.
34. Ivankovic M, Haneckova R, Thommen A, et al. Model systems for regeneration: planarians. *Development*. 2019;146(17):167684.
35. Rojo-Laguna JI, Garcia-Cabot S, Saló E. Tissue transplantation in planarians: A useful tool for molecular analysis of pattern formation. *Sem Cell Dev Biol*. 2019;87:116-124.
36. Adell T, Saló E, van Loon JJ, Auletta G. Planarians sense simulated microgravity and hypergravity. *J Biomed Biotechnol*. 2014;6:679672.
37. Morokuma J, Durant F, Williams KB, et al. Planarian regeneration in space: persistent anatomical, behavioral, and bacteriological changes induced by space travel. *Regeneration*. 2017;4(2):85-102.
38. de Sousa N, Rodriguez-Esteban G, Colagè I, et al. Transcriptomic analysis of planarians under simulated microgravity or 8 g demonstrates that alteration of gravity induces genomic and cellular alterations that could facilitate tumoral transformation. *Int J Mol Sci*. 2019;20(3):720.
39. Pezzini I, Marino A, Del Turco S, et al. Cerium oxide nanoparticles: the regenerative redox machine in bioenergetic imbalance. *Nanomedicine*. 2017;12(4):403-416.
40. Chen BH, Stephen Inbaraj B. Various physicochemical and surface properties controlling the bioactivity of cerium oxide nanoparticles. *Crit Rev Biotechnol*. 2018;38(7):1003-1024.
41. Orii H, Agata K, Watanabe K. POU-domain genes in planarian *Dugesia japonica*: the structure and expression. *Biochem Biophys Res Commun*. 1993;192(3):1395-1402.
42. Degl'Innocenti A, Rossi L, Salvetti A, et al. Chlorophyll derivatives enhance invertebrate red-light and ultraviolet phototaxis. *Sci Rep*. 2017;7(1):1-8.
43. Salvetti A, Rossi L, Iacopetti P, et al. In vivo biocompatibility of boron nitride nanotubes: effects on stem cell biology and tissue regeneration in planarians. *Nanomedicine*. 2015;10(12):1911-1922.
44. Salvetti A, Gambino G, Rossi L, et al. Stem-cell and tissue-regeneration analysis in low-dose irradiated planarians treated with cerium oxide nanoparticles. *Mater Sci Eng: C*. 2020;115:111113.
45. van Loon JJ, Krausse J, Cunha H, Goncalves J, Almeida H, Schiller P. The large diameter centrifuge, LDC, for life and physical sciences and technology. *ESASP*. 2008;553:92.
46. van Loon JJ. Some history and use of the random positioning machine, RPM, in gravity related research. *Adv Space Res*. 2007;39(7):1161-1165.
47. Borst AG, van Loon JJ. Technology and developments for the random positioning machine, RPM. *Microgravity Sci Technol*. 2009;21(4):287-292.
48. Gambino G, Falleni A, Nigro M, et al. Dynamics of interaction and effects of microplastics on planarian tissue regeneration and cellular homeostasis. *Aquat Toxicol*. 2020;218:105354.

49. Abramoff, M. D., Magalhães PJ & Ram SJ. (2004). Image processing with ImageJ. *Biophotonics Int*, 11(7), 36.
50. Eisenhoffer GT, Kang H, Alvarado AS. Molecular analysis of stem cells and their descendants during cell turnover and regeneration in the planarian *Schmidtea mediterranea*. *Cell Stem Cell*. 2008;3(3):327-339.
51. Cassella L, Salvetti A, Iacopetti P, et al. Putrescine independent wound response phenotype is produced by ODC-like RNAi in planarians. *Sci Rep*. 2017;7(1):1-17.
52. Bonuccelli L, Rossi L, Lena A, et al. An RbAp48-like gene regulates adult stem cells in planarians. *J Cell Sci*. 2010;123(5):690-698.
53. Rossi L, Cassella L, Iacopetti P, et al. Insight into stem cell regulation from sub-lethally irradiated worms. *Gene*. 2018;662:37-45.
54. Ciofani G, Genchi GG, Liakos I, et al. Effects of cerium oxide nanoparticles on PC12 neuronal-like cells: proliferation, differentiation, and dopamine secretion. *Pharm Res*. 2013;30(8):2133-2145.
55. Zhou Y, Perket JM, Zhou J. Growth of Pt nanoparticles on reducible CeO<sub>2</sub> (111) thin films: effect of nanostructures and redox properties of ceria. *J Phys Chem C*. 2010;114(27):11853-11860.
56. Bêche E, Charvin P, Perarnau D, Abanades S, Flamant G. Ce 3d XPS investigation of cerium oxides and mixed cerium oxide (Ce<sub>x</sub>Ti<sub>y</sub>O<sub>z</sub>). *Surf Interface Anal*. 2008;40(3-4):264-267.
57. Maslakov KI, Teterin YA, Popel AJ, et al. XPS study of ion irradiated and unirradiated CeO<sub>2</sub> bulk and thin film samples. *Appl Surf Sci*. 2018;448:154-162.
58. Salvetti A, Rossi L, Lena A, et al. DjPum, a homologue of *Drosophila* Pumilio, is essential to planarian stem cell maintenance. *Development*. 2005;132(8):1863-1874.
59. Pellettieri J, Fitzgerald P, Watanabe S, Mancuso J, Green DR, Alvarado AS. Cell death and tissue remodeling in planarian regeneration. *Dev Biol*. 2010;338(1):76-85.
60. Wenemoser D, Reddien PW. Planarian regeneration involves distinct stem cell responses to wounds and tissue absence. *Dev Biol*. 2010;344(2):979-991.
61. Blaber E, Sato K, Almeida EA. Stem cell health and tissue regeneration in microgravity. *Stem Cells Dev*. 2014;23(S1):73-78.
62. Ciofani G, Ricotti L, Rigosa J, Mencias A, Mattoli V, Monici M. Hypergravity effects on myoblast proliferation and differentiation. *J Biosci Bioeng*. 2012;113(2):258-261.
63. Huang Y, Dai ZQ, Ling SK, Zhang HY, Wan YM, Li YH. Gravity, a regulation factor in the differentiation of rat bone marrow mesenchymal stem cells. *J Biomed Sci*. 2009;16(1):87.
64. Rocca A, Marino A, Rocca V, et al. Barium titanate nanoparticles and hypergravity stimulation improve differentiation of mesenchymal stem cells into osteoblasts. *Int J Nanomedicine*. 2015;10:433.
65. van Loon JJ. Centrifuges for microgravity simulation the reduced gravity paradigm. *Front Astronomy Space Sci*. 2016;3:21.
66. Das S, Dowding JM, Klump KE, McGinnis JF, Self W, Seal S. Cerium oxide nanoparticles: applications and prospects in nanomedicine. *Nanomedicine*. 2013;8(9):1483-1508.
67. Rocca A, Moscato S, Ronca F, et al. Pilot in vivo investigation of cerium oxide nanoparticles as a novel anti-obesity pharmaceutical formulation. *Nanomed: Nanotechnol, Biol Med*. 2015;11(7):1725-1734.
68. Genchi GG, Degl'Innocenti A, Salgarella AR, et al. Modulation of gene expression in rat muscle cells following treatment with nanoceria in different gravity regimes. *Nanomedicine*. 2018;13(22):2821-2833.
69. Thakur N, Manna P, Das J. Synthesis and biomedical applications of nanoceria, a redox active nanoparticle. *J Nanobiotechnol*. 2019;17(1):84.
70. Pavlakov P, Dounousi E, Roumeliotis S, Eleftheriadis T, Liakopoulos V. Oxidative stress and the kidney in the space environment. *Int J Mol Sci*. 2018;19(10):3176.
71. Goodwin TJ, Christofidou-Solomidou M. Oxidative stress and space biology: an organ-based approach. *Int J Mol Sci*. 2018;23:959.
72. Steller JG, Alberts JR, Ronca AE. Oxidative stress as cause, consequence, or biomarker of altered female reproduction and development in the space environment. *Int J Mol Sci*. 2018;19(12):3729.
73. Stein TP. Space flight and oxidative stress. *Nutrition*. 2002;18(10):867-871.

#### SUPPORTING INFORMATION

Additional supporting information may be found online in the Supporting Information section at the end of this article.

**How to cite this article:** Salvetti, A., Degl'Innocenti, A., Gambino, G., van Loon, JJWA, Ippolito, C., Ghelardoni, S., Ghigo, E., Leoncino, L., Prato, M., Rossi, L., & Ciofani, G. (2021). Artificially altered gravity elicits cell homeostasis imbalance in planarian worms, and cerium oxide nanoparticles counteract this effect. *Journal of Biomedical Materials Research Part A*, 109(11), 2322-2333. <https://doi.org/10.1002/jbm.a.37215>